Supporting Online Material for

Controlled Phase Shifts With a Single Quantum Dot

Ilya Fushman, Dirk Englund, Andrei Faraon, Nick Stoltz, Pierre Petroff, Jelena Vučković*

*To whom correspondence should be addressed. E-mail: jela@stanford.edu

Published 9 May 2008, *Science* **320**, 769 (2008)
DOI: 10.1126/science.1154643

This PDF file includes:

Supporting Online Material for: Controlled Phase Shifts With a Single Quantum Dot

Ilya Fushman[1†], Dirk Englund[1†], Andrei Faraon[1†], Nick Stoltz[2]
Pierre Petroff[2], Jelena Vučković[3*]

[1]Applied Physics, Stanford University, Stanford, CA 94305

[2] Electrical and Computer Engineering, University of California, Santa Barbara, CA 93106

[3]Electrical Engineering, Stanford University, Stanford, CA 94305

[†] Authors contributed equally.

[*]To whom correspondence should be addressed. E-mail: jela@stanford.edu.

1 Experimental setup

In our measurements a strongly coupled quantum dot is identified by the QD/cavity anti-crossing signature in photoluminescence. Anti-crossing is observed by temperature-tuning a QD through the cavity resonance, using the method detailed in Ref. 1. During the temperature scan, a 980 nm diode heating laser is incident upon a metal pad next to the cavity and modulated by a triangular wave form, whose period determines the heating cycle. Both the cavity and quantum dot wavelengths shift with temperature, with the dot shifting three times faster, as shown in Fig.1C of the main text. Thus each point of the temperature scan corresponds to a particular detuning between the QD and cavity, as the system is probed at a fixed point by the resonant laser beam. This is illustrated in Fig.1, where we show how the quantum dot and cavity trajectories and phase shifts are determined. A narrow-band (5 MHz linewidth) frequency tunable external cavity diode laser is focused into the cavity and observed in cross-polarization, as detailed in

Ref.2 and shown in Fig.1A of the main texxt. The sample temperature changes from 20 to 27 K during the heating cycle. This signal beam probes the cavity-QD system at various detunings between the QD and cavity. The control beam is combined with the signal beam input path and also directed at the cavity.

2 Phase measurement theory

The system composed of the photonic crystal cavity and the distributed Bragg reflector underneath the PC membrane effectively behaves as a single-sided cavity (*2*). The detected intensity given in Eq.1 of the main text depends on the reflection coefficient for the component parallel to the cavity polarization $r(\omega)$:

$$r(\omega) = \frac{2\sqrt{\eta}\kappa}{i(\omega_{cavity} - \omega) + \kappa + \frac{g^2}{i(\omega_{QD}-\omega)+\gamma}} - 1, \tag{1}$$

The factor $\sqrt{\eta}$ accounts for the coupling efficiency into the cavity mode.

The amplitude of the signal collected after the PBS is given by $A(\theta)$, which depends on the QWP angle θ relative to the vertical polarization axis of the polarizing beam splitter as in Fig.1A of the main text. The phase of the interfering beam in Eq.1 of the main text $\Psi(\theta)$ is shown in Fig.2. This phase and amplitude of the interference term relative to the cavity signal is given in terms of θ by:

$$e^{i\Psi(\theta)} = \frac{\cos^2(2\theta) + i\sin(2\theta)}{\cos^2(2\theta) - i\sin(2\theta)}, \tag{2}$$

The amplitude at the detector is proportional to the modulus squared of $A(\theta)$, where

$$A(\theta) = \frac{i}{2}\left(\cos^2(2\theta) - i\sin(2\theta)\right), \tag{3}$$

3 Quantum dot visibility

The visibility of the QD-induced feature is reduced due to wavelength jitter (through thermal fluctuations (*2*)) as well as QD blinking between an optically active and an optically dark state. From an analysis of second-order coherence, similar to that presented in Ref.3, we deduce a dark-state probability of 25%. This limits the QD-induced features to a visibility of V=$(I_{bright} - I_{dark})/(I_{bright} + I_{dark})$=75%. With blinking and sampling taken into account, the theoretical fits agree well with experimental data. In more recent experiments, we have observed V=90% dip visibility for quantum dots that do not exhibit blinking.

4 Quantum dot saturation

The response of the quantum dot to the driving electric field is given by its susceptibility χ (*4*). This function determines the dot's radiative properties and gives the phase and amplitude of the field that interacts with the quantum dot. When the control beam is resonant with the QD, χ can be expressed as (*5*),

$$\chi = \frac{i}{1 + 4\frac{F}{(1+F)^2}\frac{P_{in}}{\gamma}} \tag{4}$$

where P_{in} is the input power, and F is the Purcell factor F=$\frac{2g^2}{\kappa\gamma}$. χ is a nonlinear function, and is typically given by an expansion in the driving electric field E as $\chi = \chi^{(1)} + \chi^{(2)}E + \chi^{(3)}E^2 + ...$ The field E is related to the input power via $P_{in}/A_{cav} = 2n_0\sqrt{\epsilon_0/\mu_0}\,|E|^2$, where $A_{cav} \approx \left(\frac{\lambda}{n_0}\right)^2$ is the cavity area, n_0 is the refractive index of GaAs and ϵ_0 and μ_0 are the dielectric constant and permeability of free space. Generally, the Kerr coefficient $\chi^{(3)}$ gives the phase modulation. Another conventional measure of nonlinearity is the intensity-dependent refractive index n_2, which is related to the Kerr coefficient via $n_2\frac{1}{10^4}\frac{P_{in}}{A_{cav}} = \frac{3\chi^{(3)}}{4n_0}\,|E|^2$ (*4*). Here the units of n_2 are cm^2/W, c is the speed of light in m/s, and $\chi^{(3)}$ is in units of m^2/V^2. A beam propagating through a cavity with such a nonlinear medium picks up a phase shift that is given

by $\phi = \frac{2\pi n_2}{\lambda}\frac{P_{in}}{A_{cav}}\frac{c}{2n_0\kappa}$. Thus, n_2 and $\chi^{(3)}$ can be determined from the change in ϕ with changes in P_{in}.

5 Computational model

The Hamiltonian for the two-beam interaction with a cavity embedded quantum dot is given by:

$$H = \hbar\omega_{QD}\sigma_z + \hbar\omega_{cav}a^\dagger a + \hbar g(\sigma_+ a + a^\dagger\sigma_-) + \sqrt{\kappa}(E_c e^{-i\omega_c t} + E_s e^{-i\omega_s t})(a + a^\dagger) \quad (5)$$

Where $\omega_{QD}, \omega_{cav}, \omega_c, \omega_s$ are the quantum dot transition frequency, cavity resonant frequency and the control and signal frequencies respectively. E_s, E_c are the control and signal driving fields respectively. The cavity photon number is given by $n_{cav} = \langle a^\dagger a\rangle$. Fits to the data were performed with the Quantum Optics Toolbox (*6*) which numerically solves this Hamiltonian with a photon number basis that ensured convergence (up to 30 photons). In the case of frequency detuned beams, a matrix continued fractions method was used to solve for the cavity mode at the signal frequency ω_s under excitation of a driving field with two frequency components ω_c, ω_s. This method expands operators in a Fourier series and solves for coefficients at the appropriate frequencies. The matlab code is available upon request.

References and Notes

1. A. Faraon, *et al.*, *Appl. Phys. Lett.* **90**, 213110 (2007).

2. D. Englund, *et al.*, *Nature* **450**, 857 (2007).

3. C. Santori, *et al.*, *Physical Review B* **69**, 205324 (2004).

4. R. Boyd, *Nonlinear Optics 2nd Edition* (Elsevier, 2003).

5. A. Auffves-Garnier, C. Simon, J. Gerard, J.-P. Poizat, *Phys. Rev. A* **75**, 053823 (2007).

6. S. Tan, *www.qo.phy.auckland.ac.nz/qotoolbox.html* .

7. Financial support was provided by the MURI Center for photonic quantum information systems (ARO/IARPA Program DAAD19-03-1-0199), ONR Young Investigator Award , NSF grant CCF-0507295. Dirk Englund and Ilya Fushman were also supported by the NDSEG fellowship. Part of the work was performed at the Stanford Nanofabrication Facility of NNIN supported by the National Science Foundation under Grant ECS-9731293.

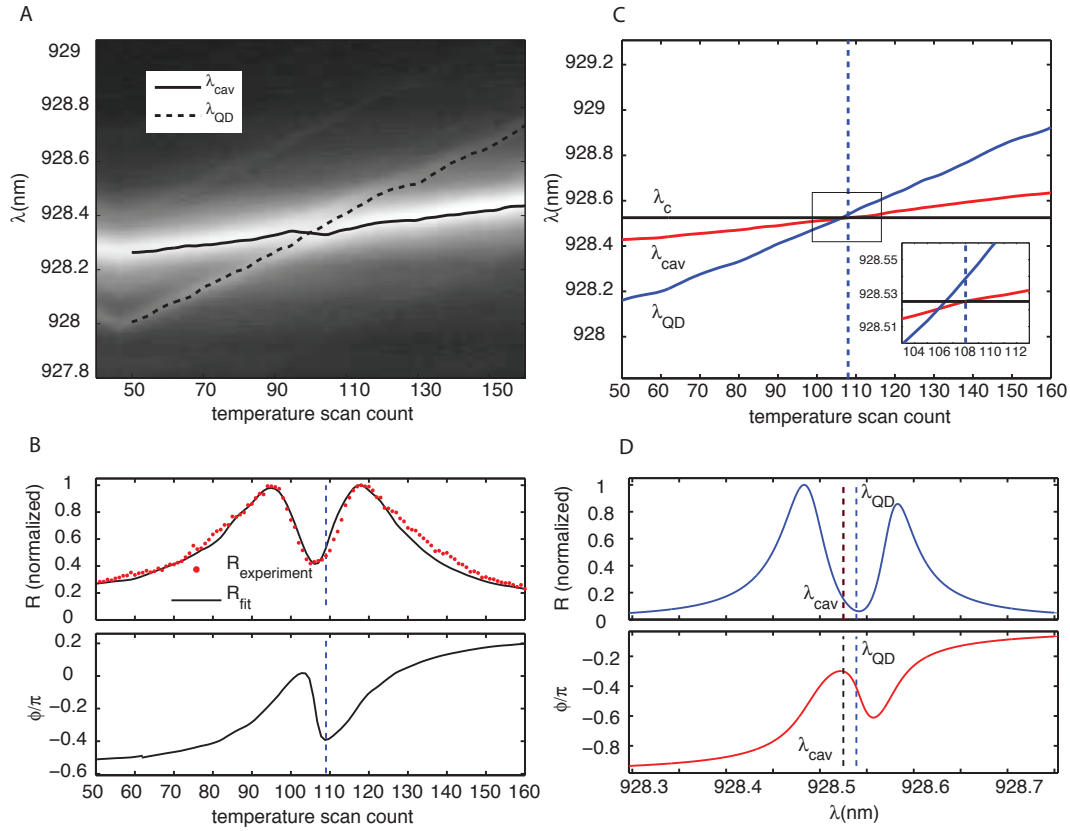

Figure 1: The quantum dot and cavity wavelengths (λ_{QD},λ_{cav}) are extracted from spectra taken as a function of the temperature scan count (A). The probing laser is positioned at a wavelength (λ_c) that is close to the point of crossing between the QD and cavity trajectories in (C). Thus, each point along the 'temperature scan count' corresponds to different offsets between the quantum dot and cavity. By tracking the amplitude of the probing laser, we can find the reflectivity signal and extract the phase in B. The point of maximum phase contrast corresponds to the vertical dashed line in B (also in C) and to a particular offset between the cavity and dot wavelengths. When the cavity and QD wavelength are fixed, and the laser is scanned along the dashed line in B, the signal shown in D would be obtained. The dot and cavity detunings are indicated by the two dashed lines. In the experiment, the laser is positioned at λ_c, which overlaps with λ_{cav} in D. The point of maximum phase contrast, which is the point where we find the phase, coincides with λ_{cav} and λ_c in this case.

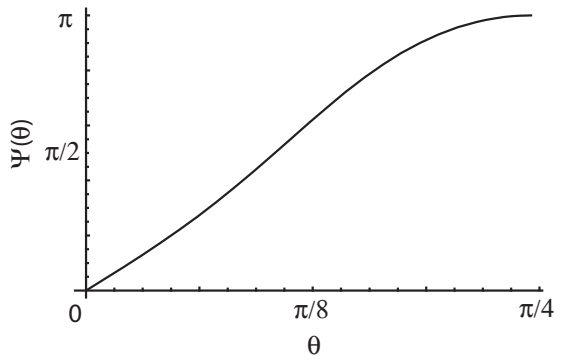

Figure 2: Phase of the interfering beam as a function of the QWP angle θ.